THE JOURNAL OF BIOLOGICAL CHEMISTRY VOL. 291, NO. 7, pp. 3626–3638, February 12, 2016

A Novel Serpin Regulatory Mechanism

*SerpinB9 IS REVERSIBLY INHIBITED BY VICINAL DISULFIDE BOND FORMATION IN THE REACTIVE CENTER LOOP**

Received for publication, October 20, 2015, and in revised form, December 2, 2015 Published, JBC Papers in Press, December 15, 2015, DOI 10.1074/jbc.M115.699298

Matthew S. J. Mangan[‡1], Catherina H. Bird[‡1], Dion Kaiserman[‡], Anthony Y. Matthews[‡], Corinne Hitchen[‡], David L. Steer[‡], Philip E. Thompson[§], and Phillip I. Bird[‡2]

From the [‡]Department of Biochemistry & Molecular Biology, Biomedicine Discovery Institute, Monash University Clayton, Clayton, Victoria 3800 Australia and the [§]Department of Medicinal Chemistry, Monash Institute of Pharmaceutical Sciences, Monash University Parkville, Parkville, Victoria 3052, Australia

The intracellular protease inhibitor Sb9 (SerpinB9) is a regulator of the cytotoxic lymphocyte protease GzmB (granzyme B). Although GzmB is primarily involved in the destruction of compromised cells, recent evidence suggests that it is also involved in lysosome-mediated death of the cytotoxic lymphocyte itself. Sb9 protects the cell from GzmB released from lysosomes into the cytosol. Here we show that reactive oxygen species (ROS) generated within cytotoxic lymphocytes by receptor stimulation are required for lyososomal permeabilization and release of GzmB into the cytosol. Importantly, ROS also inactivate Sb9 by oxidizing a highly conserved cysteine pair (P1-P1′ in rodents and P1′-P2′ in other mammals) in the reactive center loop to form a vicinal disulfide bond. Replacement of the P4-P3′ reactive center loop residues of the prototype serpin, SERPINA1, with the P4-P5′ residues of Sb9 containing the cysteine pair is sufficient to convert SERPINA1 into a ROS-sensitive GzmB inhibitor. Conversion of the cysteine pair to serines in either human or mouse Sb9 results in a functional serpin that inhibits GzmB and resists ROS inactivation. We conclude that ROS sensitivity of Sb9 allows the threshold for GzmB-mediated suicide to be lowered, as part of a conserved post-translational homeostatic mechanism regulating lymphocyte numbers or activity. It follows, for example, that antioxidants may improve NK cell viability in adoptive immunotherapy applications by stabilizing Sb9.

Serpins comprise a family of protease inhibitors found in all kingdoms of life that act by presenting an exposed reactive center loop (RCL)[3] to the target protease, which then cleaves the peptide bond between two residues designated P1 and P1′. This triggers a conformational change in the serpin, irreversibly trapping the protease in a covalently bound complex (1, 2). Residues around the P1 contribute to protease binding, and alteration of a serpin RCL by mutation can abrogate inhibition or alter target specificity (3). *In vitro* experiments also show that chemical modification can inactivate a serpin (4).

Sb9 (SerpinB9) is an intracellular inhibitor of the mammalian cytotoxic lymphocyte (CL) serine protease, GzmB (granzyme B) (5–7). GzmB is mainly produced by $CD8^+$ T cells and natural killer (NK) cells and is stored in lysosome-related organelles (cytotoxic granules) prior to perforin-mediated release into a target cell. Sb9 is expressed in the nucleocytoplasm of $CD8^+$ T cells and NK cells and in dendritic cells. During an immune response, Sb9 protects effector and accessory cells from apoptosis induced by ectopic GzmB (6, 8–10). This is exemplified by mice lacking Sb9, which have lower than normal numbers of virus-specific $CD8^+$ T cells during infection with lymphocytic choriomeningitis virus. By contrast, mice lacking both Sb9 and GzmB have normal numbers of virus-specific $CD8^+$ T cells, implicating uncontrolled GzmB as a mediator of $CD8^+$ T cell disappearance (11). GzmB-mediated death has also been reported in responding invariant NKT cells, helper T cell, and regulatory T cells (12, 13). The pathophysiological importance of GzmB in immune cell homeostasis is also exemplified by decreased death of GzmB-null Th2 $CD4^+$ T helper cells (14). These cells have longer life spans than normal, resulting in a skewed cytokine response *in vivo* and an increase in the allergic immune response (14). Overall, such data suggest that the GzmB-Sb9 axis plays an important role in the maintenance of immune cell populations.

For GzmB to cause apoptosis of CLs during an immune response, it must access the CL cytosol. It could be delivered from a neighboring cell (fratricide), as observed in Sendai virus infection where regulatory T cells limit effector $CD8^+$ T cell life span by killing these cells in a GzmB- and perforin-dependent manner (15, 16). Alternatively, it can be released from the cytotoxic granules of the CL if they are destabilized and undergo lysosomal membrane permeabilization (LMP). LMP in CLs has been demonstrated following engagement of either CD2 or CD16 on NK cells or CD3 restimulation of activated $CD8^+$ T cells, resulting in translocation of GzmB to the cytosol and GzmB-mediated death (17–19). Damaged lysosomes are evident in NK cells conjugated to targets, and CLs lacking Sb9 are more sensitive to LMP-associated death (19).

* This work was supported by the National Health and Medical Research Council of Australia. The authors declare that they have no conflicts of interest with the contents of this article.

[1] These authors contributed equally to this work.

[2] To whom correspondence should be addressed: Dept. of Biochemistry & Molecular Biology, Monash University, Wellington Rd., Clayton, Victoria 3800, Australia. Tel.: 61-3-99029365; Fax: 61-3-99029500; E-mail: phil.bird@monash.edu.

[3] The abbreviations used are: RCL, reactive center loop; ROS, reactive oxygen species; CL, cytotoxic lymphocyte; NK, natural killer; LMP, lysosomal membrane permeabilization; 2-ME, β-mercaptoethanol; MnTBAP, manganese (III) tetrakis (4-benzoic acid) porphyrin chloride; AO, acridine orange; LLOMe, Leu-Leu-methyl-ester; LSB, Laemmli sample buffer; K-dnp, dinitrophenyllysine; A1AT, α_1-antitrypsin; AICD, activation-induced cell death; SI, stoichiometry of inhibition.

It is generally accepted that LMP is caused by a variety of stressors, including reactive oxygen species (ROS) (20). Receptor engagement in CLs increases intracellular ROS production from mitochondria and NADPH oxidases, which is required for correct activation of the cell (21, 22) and the control of life span by modulating transcription of pro- and anti-apoptotic factors (23). Although ROS function as essential second messengers in CLs (24), they also alter the intracellular environment by modifying lipids, proteins, and nucleic acids and by damaging organelles. ROS can also come from the external environment, generated by neighboring neutrophils and macrophages (25).

Here we demonstrate an additional role for ROS in CLs, namely in promoting GzmB-mediated death via induction of LMP and inactivation of Sb9. ROS promotes GzmB release from lysosomes into the cytoplasm and also oxidizes highly conserved Cys residues in the RCL of Sb9 preventing it from interacting with GzmB. As a consequence of Sb9 inactivation, the CL becomes more sensitive to LMP and GzmB-mediated death. ROS-mediated LMP coupled to suppression of Sb9 may therefore be an important factor in an emerging cell autonomous mechanism that controls CL (and other immune cell) life span (19).

Experimental Procedures

Cell Culture—The human NK-like cell line YT and human T cell-like cell line Jurkat E6.1 were cultured in RPMI 1640 supplemented with 10% heat-inactivated fetal calf serum, 2 mM L-glutamine, 50 units/ml penicillin, 50 μg/ml streptomycin, and 90 μM β-mercaptoethanol (2-ME) (RPMI-10). NK92 cells grown in Iscove's modified DMEM supplemented as for YT cells. HeLa cells were in DMEM supplemented as for YT cells. Human NK cells were isolated as described and grown in RPMI-10 with 1 mM sodium pyruvate and 0.1 mM nonessential amino acids (RPMI-CL) (19). Human $CD8^+$ T cells were isolated on the basis of CD8 expression from NK-depleted mononuclear cells obtained from peripheral blood, grown in RPMI-CL, and activated by adding 5 μg/ml concanavalin A (Sigma-Aldrich) and 100 units/ml IL-2 for 3 days. Purified CTLs were 70.11 $\pm$ 13.90% CD3+ and 74.14 $\pm$ 8.01% $CD8^+$. Mouse CTL were generated from splenocytes obtained from C57BL/6 (WT), GzmB KO, or Sb9 KO mice and activated with 0.1 mg/ml anti-CD3 and anti-CD28, 100 units/ml IL-2, and 2 ng/ml IL-7 for 3 days as described previously (19). For treatment with H_2O_2 (Sigma-Aldrich), the cells were washed twice into RPMI-CL without 2-ME and incubated in media containing H_2O_2 for 30 min at 37 °C.

Treatment of NK Cells with ROS Indicators or Inhibitors—NK cells from human peripheral blood were activated in medium containing 100 units/ml IL-2 for 4 days. 1×10^6 cells in 1 ml were pretreated for 2 h with 5 mM Tiron (Sigma), 1.25 mM *N*-acetylcysteine (Sigma), 1 mM or 10 mM deferroxamine (Sigma), 10 μM diphenylene iodonium (Sigma) or 200 μM manganese (III) tetrakis (4-benzoic acid) porphyrin chloride (MnTBAP; Calbiochem). CD2 and CD16 receptor stimulation by antibody cross-linking was as described (19). 2′,7′-dichlorodihydro-fluorescein diacetate (Sigma) was used at 30 μM. The cells were cultured in complete medium containing 5 μg/ml acridine orange (AO; MP Biomedicals) for 15 min prior to lysosomal disruption. Changes in AO distribution were determined by FACS analysis using FL1 to monitor cytosolic AO and FL3 to measure lysosomal AO.

Induction of LMP in NK Cells—Medium lacking 2-ME was used throughout this experiment. YT cells cultured overnight were transferred to fresh medium supplemented with 10 mM HEPES (pH 7.2) at a density of 1×10^6 cells/ml. The cells were pretreated as indicated with 10 mM C20 for 2 h. Appropriate samples were exposed to 40 μM H_2O_2 for 10 min before addition of 125 μM Leu-Leu-methyl ester (LLOMe). Cell morphology and viability was examined by trypan blue staining after 45 min of incubation. Trypan blue-negative cells with unaltered morphology were scored as viable; trypan blue-positive cells with clear membrane blebbing were scored as dying; trypan blue-negative cells were scored as dead.

Lentivirus Production and Transduction—The lentiviral vector pLox-dsRed was constructed by replacing the SmaI-NheI EGFP-encoding fragment from the lentiviral vector pLOX/EWgfp (Addgene) with the SmaI-XbaI fragment from pIRES2-dsRED-Express (Clontech) containing the IRES-dsRed element. An EcoRI fragment containing either the human or mouse Sb9 coding sequence was then inserted into the EcoRI site of pLox-dsRed. An extension-overlap PCR approach was used to convert the two Cys residues to Ser in the human or mouse Sb9 RCL (SS mutants). The mutagenic primers were 5′-GCAGAGAGCTCCATGGAATCTG-3′ and complement (human) and 5′-CATCATAGAATTCTCGAGTGCCTCTTC-3′ and complement (mouse). The human flanking primers were 5′-GGGGATCCATGGAAACTCTTTCTAATGC-3′ and 5′-GGGGATCCTTATGGCGATGAGAACC-3′. Mouse flanking primers were 5′-GGGGATCCATGAATACTCTGTCTGAAGG-3′ and 5′-GGGGATCCTTATGGAGATGAGAACCTGCCAC-3′. Mutated products were cloned into pZero-Blunt (Invitrogen) and sequenced, then the plasmid was cleaved with BamHI to release the Sb9 fragment which was inserted into the unique BamHI site of pLox-dsRed. Lentivirus was produced as described (26) via co-transfection of HEK-293T cells with a pLox-ds-Red construct and packaging plasmids pMD2G and psPAX2 (Addgene). Jurkat cells were plated in a flat-bottomed 96-well tray at 3×10^4 cells/well in RPMI-10 containing 8 μg/ml Polybrene and lentivirus particles (multiplicity of infection, 5–10; total volume, 100 μl). The cells were then centrifuged at 1500 $\times$ *g* for 45 min at 30 °C. Following centrifugation, 100 μl of RPMI-10 was added to each well, and the cells were incubated for 48 h. The cells were assessed for expression of the transduced gene by analyzing dsRed expression via FACS. After expansion, the positive cells from each transduction were sorted into populations expressing comparable levels of dsRed. Immunoblotting confirmed equivalent levels of Sb9 expression (data not shown).

Antibodies—We used hamster anti-mouse CD3 (145-2C11; BD Biosciences); hamster anti-mouse CD28 (37.51; BioLegend); rabbit polyclonal antibodies to recombinant human Sb9 (5) or recombinant mouse Sb9 (Jomar Bioscience); mouse anti-human Sb9 (7D8) (27); mouse anti-human GzmB for immunoblotting (2C5) (28); rat anti-mouse GzmB for immunoblotting (16G6; eBioscience); goat anti-actin (Santa Cruz Biotechnology); mouse anti-β tubulin (AA2; EMD Millipore);

and species-specific HRP-conjugated secondary antibodies (Rockland Immunochemicals, Gilbertsville, PA).

Cell Extracts and Immunoblotting—Serpin/serine protease complexes are SDS stable and can be visualized by immunoblotting following separation via SDS-PAGE. For analysis of Sb9 function, complexes were allowed to form postlysis. The cells were lysed in ½ volume Nonidet P-40 lysis buffer (1% (v/v) Nonidet P-40 in 50 mM Tris, pH 8.0, 10 mM EDTA, pH 8.0, 150 μg/ml PMSF, 1 μg/ml aprotinin, 0.5 μM leupeptin, and 1 μM pepstatin) and incubated at 37 °C for 10 min to facilitate complex formation. ½ volume of 2× Laemmli sample buffer (LSB) was then added to halt the reaction. Cell extracts for analysis of protein without allowing postlysis complex formation were prepared by directly lysing cells in LSB. Any complexes detected under these conditions are formed within the cell, prelysis. Samples were resolved by SDS-PAGE and transferred to nitrocellulose membranes for immunoblotting and visualization via chemiluminescence.

Synthesis of Quenched Fluorescence Peptide Substrates—Substrates based on the RCL of Sb9 incorporating the fluorophore anthranilic acid and fluorescence quencher dinitrophenyllysine (K-dnp) were synthesized as described (29). These included the human GzmB substrates Abz-VVAECCMES[K-dnp]S, Abz-VVAECSMES[K-dnp]S, Abz-VVAECSMES-[K-dnp]S, and Abz-VVAESSMES[K-dnp]S and the mouse GzmB substrates Abz-IEFCCASS[K-dnp]S, Abz-IEFCSASS[K-dnp]S, and Abz-IEFSSASS[K-dnp]S. The substrates used in kinetic analyses were purchased from Mimetopes: Abz-VVADSS[K-dnp]S or Abz-IEPDSGSQ[K-dnp] (human GzmB) or Abz-LEYDLGAL[K-dnp] (mouse GzmB) (8).

Granzyme B Activity Assays—1×10^7 cells were lysed in Triton X-100 lysis buffer (1% Triton (v/v) in PBS) and lysates diluted in TBS to ~9 mg/ml. Quenched fluorescence peptide substrates (Abz-IEPDSSMESK-dnp or Abz-LEYDLGALK-dnp) were added to 100 μl of cell extract, and GzmB activity was assayed using a fluorescence plate reader (FLUOstar OPTIMA; BMG LABTECH). To measure recombinant GzmB activity, peptide substrates were diluted into TBS containing either 5 mM 2-ME or 100 μM H_2O_2 and incubated at 37 °C for 10 min. GzmB was added, and the activity on the substrate was assayed as above. Where indicated, cells were preincubated with the selective human GzmB inhibitor compound 20 (C20) (19) at 40 μM for 5 min at 37 °C prior to substrate addition.

Serpin-Protease Complex Formation Assay—Protease and serpin were mixed together at the indicated ratio and incubated for 37 °C for 10–40 min to facilitate complex formation. For experiments assessing complex formation under different oxidative conditions, the protein was first dialyzed against TBS containing either 100 μM H_2O_2 or 5 mM 2-ME.

Mass Spectrometry Measurement—Assay samples were co-spotted onto the MALDI target plate with Matrix solution of 10 mg/ml α-cyano-4-hydroxycinnamic acid (Laser BioLabs, Sophia-Antipolis, France) in 50% acetonitrile, 0.1% TFA. The samples were analyzed on an Applied Biosystems (Foster City, CA) 4700 Proteomics Analyzer MALDI TOF/TOF in Reflectron mode with a mass range of 1000–4000 Da, focus mass of 1500 Da at 2000 shots per spectra. The spectra were calibrated using the default calibration that was updated by the plate model method against 4700 peptide mix immediately prior to sample acquisition. The data were processed using the 4700 Series Explorer software.

Recombinant Protein Production—The hybrid Sb9-α_1-antitrypsin (SERPINA1 (A1AT)) serpin was constructed by replacing the P4-P3′ residues of the human A1AT RCL with the P4-P5′ residues of the Sb9 RCL using a PCR extension/overlap strategy. The template plasmid carried the human A1AT gene modified to remove the signal sequence and include six His residues and TEV cleavage site immediately after the initiation codon. The mutagenic primers were 5′-GTAGTTGCAGAGTGCTGCATGGAATCTCCCGAGGTCAAGTTCAACAAACCC-3′ (sense) and 5′-AGATTCCATGCAGCACTCTGCAACTACCTCTAAAAACATGGCCCCTGC-3′. The flanking primers were 5′-TCTGCCATCATGAGAGGATCTCACCATCACC-3′ (sense) and 5′-GAGGCAGTTATTTTTGGGTGGG-3′ (antisense). The resulting chimeric product was cloned into pZeroBlunt, verified by DNA sequencing, and then cloned using EcoRI into the *Pichia pastoris* expression vector, pHILD2. Purification of the hybrid Sb9-A1AT serpin, or Sb9 and variants, from *P. pastoris* was as described (30). Hexahistidine tags were removed by TEV protease.

Human GzmB was produced as described in Ref. 31. The zymogen form of mouse GzmB was modified to replace the signal peptide and prodomain with a His_6 tag and bovine enterokinase cleavage site and cloned into the *Escherichia coli* expression plasmid pEXP-His. Recombinant protein was expressed in inclusion bodies in BL21 arabinose-inducible *E. coli*. These were collected by centrifugation of the lysed bacterial pellet and washed three times: wash 1 contained 25 mM Tris, pH 7.4, 2 mM EDTA, 20 mM DTT, 1% (v/v) Triton X-100; wash 2 contained 25 mM Tris, pH 7.4, 2 mM EDTA, 1 M NaCl; and wash 3 contained 25 mM Tris, pH 7.4, 2 mM EDTA. The insoluble protein pellet was collected and denatured in 7 M guanidine, 100 mM DTT, and 100 mM Tris, pH 8.3. The denatured protein was refolded by slow, dropwise addition into 50 mM Tris, pH 7.4, 1 mM EDTA, 1 mM L-Cys, 3 mM L-cystine, 600 mM L-arginine, 500 mM NaCl, and 10% (v/v) glycerol. The solution containing soluble and correctly folded pro-granzyme was concentrated by tangential flow filtration before activation with bovine enterokinase as described previously (31). Mature GzmB was collected using a SP-Sepharose Fast Flow HiTrap FPLC column (GE Biosciences), eluted with an increasing NaCl gradient.

Serpin and Substrate Kinetics—Both the stoichiometry of inhibition (SI) and association constant (k_{ass}) were measured and calculated according to Ref. 32, using the substrate Abz-VVADSS[K-dnp]S (human). Kinetics of peptide substrate cleavage were determined as in Ref. 33.

Results

ROS Promote LMP and GzmB-mediated CL Death—We have previously shown that LMP is associated with activation-induced cell death (AICD) of CTL following CD3 restimulation or AICD of NK cells following CD2 or CD16 ligation. This is evident via loss of lysosomal membrane integrity and appearance of GzmB in the cytosol (19). Using a GzmB-eGFP fusion protein that is directed to the CL lysosome, we have also

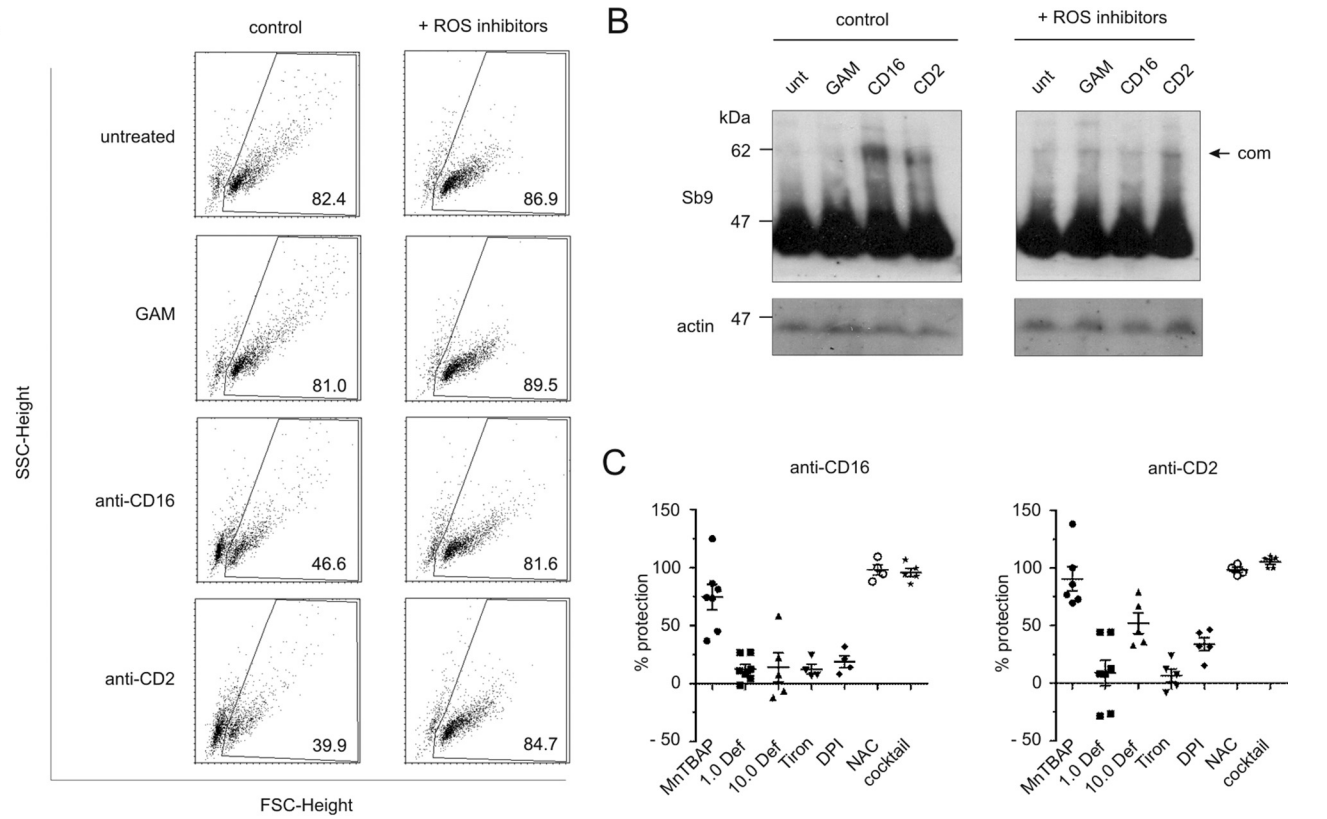

FIGURE 1. **ROS participate in receptor-stimulated death of CLs.** *A*, activated primary human NK cells were untreated or pretreated for 2 h with a mixture of ROS inhibitors: Tiron, *N*-acetylcysteine (*NAC*), deferroxamine (*Def*), diphenylene iodonium (*DPI*), or MnTBAP. To drive receptor-stimulated death, cells were then exposed for 2 h to anti-CD2 or anti-CD16 antibodies cross-linked with goat anti-mouse (*GAM*) antibody or to goat anti-mouse antibody alone (inhibitors remained in the medium) and then analyzed by FACS using forward light scatter (*FSC*) and side light scatter (*SSC*) for cell survival or lysed in LSB for immunoblotting. Gated cells represent the viable population, and the percentage of survival is indicated for each experiment. *B*, the LSB lysates were resolved by 10% SDS-PAGE, and proteins were transferred to nitrocellulose for immunoblotting. The membrane was probed sequentially for Sb9 (R11 antibody) and actin. An *arrow* indicates the Sb9/GzmB complex (*com*). *C*, activated NK cells were treated as in *A* with individual ROS inhibitors or the mixture, and cell survival was determined by FACS analysis. The protection conferred by treatment with each ROS inhibitor was calculated relative to cells treated with GAM alone. Each point represents an independent experiment. The *error bars* indicate S.E.

observed that *in vitro* ROS treatment of CLs perturbs lysosomes and causes LMP and death of the CLs (34).

We therefore investigated whether ROS are associated with AICD and release of GzmB into the cytosol. As previously described (19), treatment of NK cells with either anti-CD2 or anti-CD16 leads to cell death (Fig. 1*A*) and appearance of GzmB in the cytosol as indicated by the formation of a complex with cytoplasmic Sb9 (Fig. 1*B*). (The cells were lysed in SDS, which prevents postlysis binding of GzmB and Sb9; complex formation is then a direct indicator of GzmB release from lysosomes into the cytoplasm (8).) Strikingly, both complex formation and cell death were abrogated by pretreatment with a mixture of ROS inhibitors (Fig. 1, *A* and *B*), strongly implicating ROS as a second messenger in AICD. In subsequent experiments, we evaluated the effect of the individual inhibitors in the mixture, observing almost complete protection by *N*-acetylcysteine or MnTBAP against anti-CD2 and anti-CD16 stimulation and partial protection by deferroxamine and diphenyl iodonium against anti-CD2 stimulation (Fig. 1*C*). We concluded that ROS generated following receptor stimulation are essential for initiation of LMP and cell death.

Receptor stimulation is fundamental to CL cytotoxicity, and we have previously shown that NKs conjugated with target cells have damaged lysosomes (19). To demonstrate that ROS are generated in working NKs during target cell conjugation and killing, we compared unconjugated and conjugated NK cells preloaded with the ROS indicator 2′7′-dichloro-dihydro-fluorescein diacetate via flow cytometry (Fig. 2*A*). This showed that NK cells on targets produce considerably more ROS, which might contribute to LMP. To demonstrate that ROS can promote LMP in CLs, we used the AO translocation assay (34) to assess CLs treated with increasing concentrations of H_2O_2. (H_2O_2 was used as an oxidant in this study because it is normally produced by immune cells and so provides a biologically relevant model ROS.) FACS analysis showed a direct, dose-dependent relationship between H_2O_2 and the accumulation of AO in the CL cytoplasm (Fig. 2*B*). Assessment of these ROS-treated CLs by epifluorescence microscopy showed significant perturbation of the lysosomal compartment and evidence of transfer of lysosomal contents into the cytoplasm (Fig. 2*B*). Furthermore, examination of extracts from H_2O_2-treated cells showed appearance of GzmB-Sb9 complexes, gradually increasing with H_2O_2 concentration (Fig. 2*C*). No complexes were evident in untreated cells. Samples of treated cells analyzed in parallel showed visual evidence of lysosomal perturbation and release of AO into the cytosol at relatively low H_2O_2 concentrations (Fig. 2*C*).

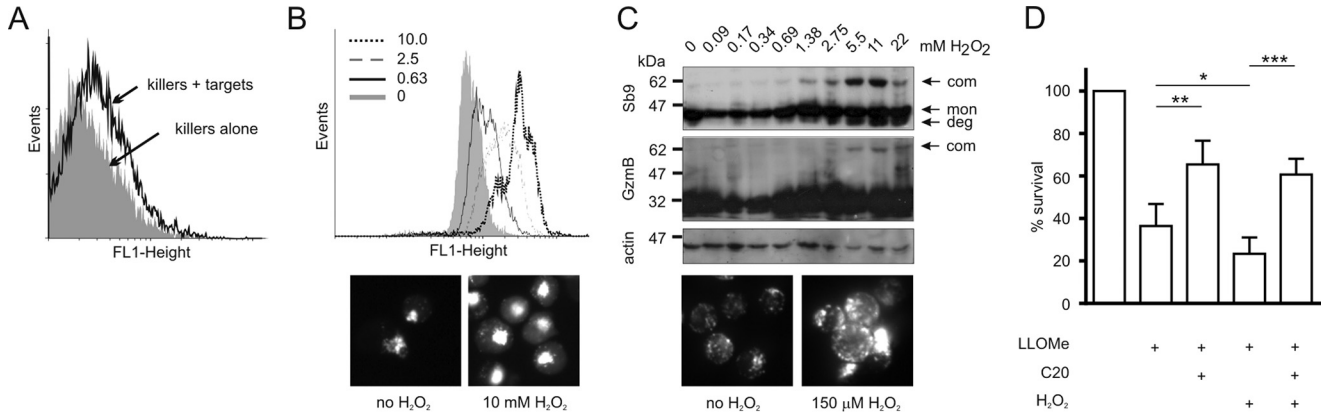

FIGURE 2. **ROS cause LMP, release of GzmB, and death of CLs.** *A*, NK92 cells preincubated for 15 min in 2′,7′-dichloro-dihydro-fluorescein diacetate were mixed with HeLa target cells at 1:1 for 1 h. The cells were then washed and analyzed by FACS. *B*, YT cells pretreated with AO were exposed to the indicated concentrations of H_2O_2 for 30 min, and AO translocation was assessed by FACS. Separately, YT cells were loaded with AO for 15 min, washed, and exposed to 10 mM H_2O_2 for 30 min prior to microscopy. *C*, serial 2-fold dilutions of H_2O_2 were mixed with an equal volume of NK92 cells (2×10^6 cells/ml) and incubated for 1 h, and then cells were lysed in SDS. Samples equivalent to 2×10^5 cells/lane were resolved via 10% SDS-PAGE and immunoblotted sequentially for GzmB (2C5), actin, and Sb9 (R11). NK92 cells were separately loaded with AO for 15 min and exposed to 150 μM H_2O_2 for 30 min prior to microscopy. *Arrows* and labels indicate the Sb9/GzmB complex (*com*), unbound Sb9 (*mono*), and complex degradation products or cleaved Sb9 (*deg*). *D*, 1×10^6 YT cells/ml were pretreated with 40 μM H_2O_2 for 10 min before addition of 125 μM LLOMe. Some cells were also pretreated with 10 mM C20 for 2 h. Cell morphology and viability was examined by trypan blue staining after 45 min of incubation. Each experiment was performed a minimum of three times, and pooled data are shown as bar graphs of mean and S.D.

The data described above clearly suggest that ROS mediate LMP; however, we wondered whether ROS influence other factors participating in AICD. To this end, CLs were briefly treated with a low, non-LMP-inducing concentration of H_2O_2 prior to initiating LMP using the well characterized lysosomotropic agent LLOMe (19). As shown in Fig. 2*D*, ~60% of cells treated with LLOMe alone died, but ~80% died if pretreated with H_2O_2. This suggests that ROS inhibit a cytoprotective factor, as well as destabilizing lysosomes. Cell survival markedly improved in the presence of compound 20 (C20), a specific, cell-permeable inhibitor of GzmB, confirming that GzmB is an important effector of LMP-mediated death as previously reported (19). An obvious candidate for a ROS-sensitive cytoprotective factor is therefore Sb9.

SerpinB9 Is Partially Inactive in Primary T Cells—Phylogenic analyses have suggested that Sb9 arose in mammals, because it is absent from birds, amphibians, and fish (35, 36). Our further analysis showed it is evident in Eutheria (placental mammals) and is absent from Prototheria (monotremes) (data not shown). In all Eutherian orders and almost all families, the Sb9 RCL contains two adjacent Cys residues (Fig. 3*A*). (The exception is the Bovidae family Sb9 (cow), but because this serpin has a predicted P1 Asp (instead of Glu/Cys), it may target caspases rather than GzmB (6) and is unlikely to be a true ortholog.) In most species, these RCL Cys residues comprise the P1′ and P2′ residues immediately downstream of the P1 Glu (33), but in rodents they comprise the P1-P1′ residues (8). Given the well known susceptibility of Cys to oxidation, it is possible that modification of these residues prevents interaction with GzmB and decreases CL viability following LMP. If so, and because ROS are essential for activation and proliferation of T cells (37), it follows that a proportion of the Sb9 pool in proliferating T cells will be oxidized and inactivated by ROS.

In CLs, the amount of GzmB stored in lysosomes exceeds the levels of cytosolic Sb9. As previously reported (8) and illustrated in Fig. 3*B*, when all the lysosomal GzmB in a CL is released into the cytosol by lysing cells in Nonidet P-40 detergent (instead of SDS), functionally competent serpin molecules immediately move into a postlysis complex with GzmB. In uncompromised cells, most if not all the serpin enters complexes (Fig. 3*B*). To test whether Sb9 is fully functional in primary T cells, its ability to complex with GzmB postlysis was assessed. Activated, proliferating $CD8^+$ T cells from peripheral human blood were lysed in Nonidet P-40 to allow postlysis binding of GzmB to Sb9. A parallel sample of cells was lysed in SDS to prevent postlysis binding of GzmB and Sb9 (8). Extracts were then analyzed by SDS-PAGE and immunoblotting (Fig. 3*C*). In the SDS lysates, uncomplexed Sb9 (42 kDa) and GzmB (28 kDa) predominated, indicating that there is normally little or no release of GzmB into the cytosol of these cells. In the Nonidet P-40 samples, where postlysis binding was allowed to occur, a 62-kDa complex between GzmB and Sb9 was evident, along with complex degradation products. Importantly, significant amounts of uncomplexed 42-kDa Sb9 were evident, suggesting that not all Sb9 molecules are functional in these cells. Incubation of the Nonidet P-40 lysates for longer did not increase the amount of complex formed (data not shown). To ensure that GzmB was not a limiting factor, some cells were lysed in Nonidet P-40 containing added recombinant human GzmB. This removed one of the degradation species (proteolyzed by the added GzmB) but did not increase complex formation or reduce the amount of unbound serpin, confirming that not all Sb9 in these T cells is functional.

To determine whether this observation is also true for mouse Sb9, the experiment was repeated using primary activated murine T cells (Fig. 3*D*). The cells were assessed for GzmB-Sb9 complex formation as described above. As with human Sb9, a proportion of mouse Sb9 failed to complex with GzmB. To ensure that the lack of complete interaction was not due to limiting GzmB, T cells lacking GzmB were lysed in Nonidet P-40 containing added recombinant mouse GzmB. Some Sb9 still failed to move into complex, indicating that it is inactive.

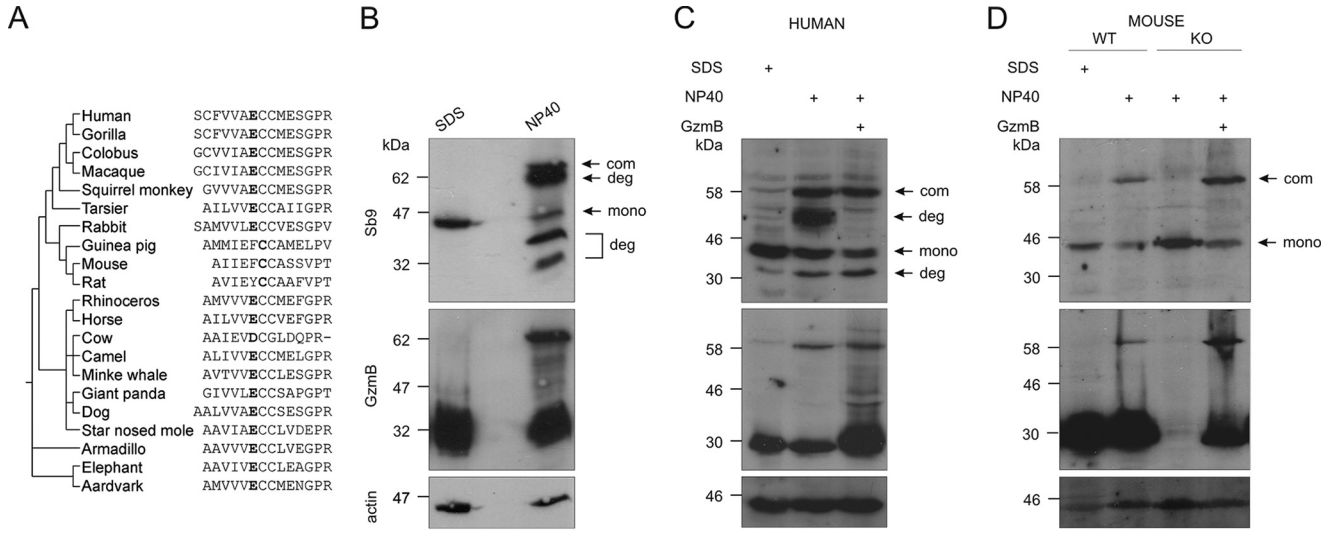

FIGURE 3. **Sb9 is not fully functional in primary CLs.** *A*, dual Cys residues are conserved in the Sb9 RCL. Amino acid sequence alignment of Sb9 RCLs. The putative P1 residue is indicated in *bold type*. The P1-P1′ cleavage site has been confirmed in human (33) and mouse (8). *B*, cell disruption by Nonidet P-40 but not SDS detergent allows postlysis formation of Sb9 and GzmB complexes. 2×10^5 YT cells/lane were solubilized in Nonidet P-40 lysis buffer or SDS (LSB) prior to 12.5% SDS-PAGE and sequential immunoblotting for human Sb9 (R15, 1:2000), GzmB (2C5, 1:100), or actin (1:1000). *C*, Sb9 activity in activated human CTL. 5×10^5 cells/lane were lysed in SDS or in Nonidet P-40 in the presence of recombinant GzmB, resolved via 10% SDS-PAGE, and immunoblotted as in *B*. *D*, Sb9 activity in activated mouse CTL from WT or GzmB KO mice. 5×10^5 cells/lane were processed as in *C*, and the immunoblot was sequentially probed for mouse Sb9 (1:1000), GzmB (16G6, 1:1000), and actin. *Arrows* and labels indicate the Sb9/GzmB complex (*com*), unbound Sb9 (*mono*), and complex degradation products or cleaved Sb9 (*deg*).

Taken together, these results are consistent with ROS-mediated inactivation of a proportion of Sb9 in proliferating T cells.

Complex Formation between GzmB and Sb9 Is Reversibly Inhibited by ROS—To confirm that oxidation disrupts the interaction between Sb9 and GzmB, a human NK-like cell line, YT, was treated with H_2O_2. Nonidet P-40-generated YT cell lysates were incubated to facilitate formation of complex, which was assessed by immunoblotting. In extracts from untreated cells, essentially all the Sb9 bound to GzmB and moved into complex, indicating that Sb9 is functional (Fig. 4*A*). Treatment of the cells with H_2O_2 substantially reduced Sb9-GzmB complex and increased free Sb9, indicating that the interaction is susceptible to ROS (Fig. 4*A*).

Proteins can undergo a variety of oxidative modifications, which can be broadly classed as either reversible or irreversible. Irreversible modifications generally indicate protein damage, whereas reversible modifications are often involved in signal transduction and control the activity of some proteins (38). To determine whether the modification occurring in this case is reversible, H_2O_2-treated YT cells were lysed in Nonidet P-40 containing 100 μM of the reductant DTT. Lysis of the cells in the presence of DTT fully restored complex formation (Fig. 4*A*).

To ascertain whether complex formation between mouse Sb9 and GzmB is similarly affected by oxidation, activated mouse splenocytes were treated with 500 μM H_2O_2 and lysed in Nonidet P-40 to assess complex formation. As also shown above (Fig. 3*D*), not all mouse Sb9 is active in these cells; however, exposure to H_2O_2 clearly decreased the amount of complex formed (Fig. 4*A*). Lysis of H_2O_2-treated cells in DTT restored complex formation (Fig. 4*A*). These results established that a reversible oxidative modification prevents complex formation between Sb9 and hGzmB.

Oxidation Inhibits Sb9 but Not GzmB—Loss of interaction between Sb9 and hGzmB by ROS could be due to modification of Sb9, GzmB, or both. To distinguish between these possibilities, YT cells treated with 500 μM H_2O_2 were lysed in the presence or absence of recombinant Sb9 (Fig. 4*B*). As also shown in Fig. 4*A*, Sb9 complexes were markedly reduced in H_2O_2-treated cells. Complex formation increased on addition of recombinant Sb9 to cytosolic extracts from the H_2O_2-treated cells, confirming that the residual endogenous Sb9 was inactive (Fig. 4*B*). A larger proportion of endogenous GzmB moved into complex when recombinant Sb9 was added, suggesting that GzmB is unaffected by oxidation (data not shown). To confirm this, GzmB activity was assessed in cytosolic extracts from untreated or H_2O_2-treated YT cells using a quenched fluorescence peptide substrate cleavage assay. Specificity of cleavage of the substrate was demonstrated by adding a potent GzmB inhibitor, compound 20 (39), to parallel samples. GzmB specific activity was unchanged in H_2O_2-treated cells, confirming that GzmB is not affected by ROS (Fig. 4*C*).

To determine whether mouse Sb9 or GzmB undergo oxidative modification, activated splenocytes from WT mice were treated with 500 μM H_2O_2 and lysed in the presence of recombinant mouse Sb9. H_2O_2 completely abolished complex formation, which was restored by the addition of recombinant Sb9 to the cell extract (Fig. 4*B*). The activity of GzmB in these extracts was assessed via quenched fluorescence substrate cleavage. T cells generated from the GzmB KO mouse were used to confirm the specificity of the substrate; cleavage was mostly due to GzmB because there was only 30% of the activity present in the lysates from the GzmB KO cells (Fig. 4*C*). H_2O_2 treatment did not alter GzmB activity in WT cell extracts, illustrating that mouse GzmB is not sensitive to oxidation (Fig. 4*C*). Overall

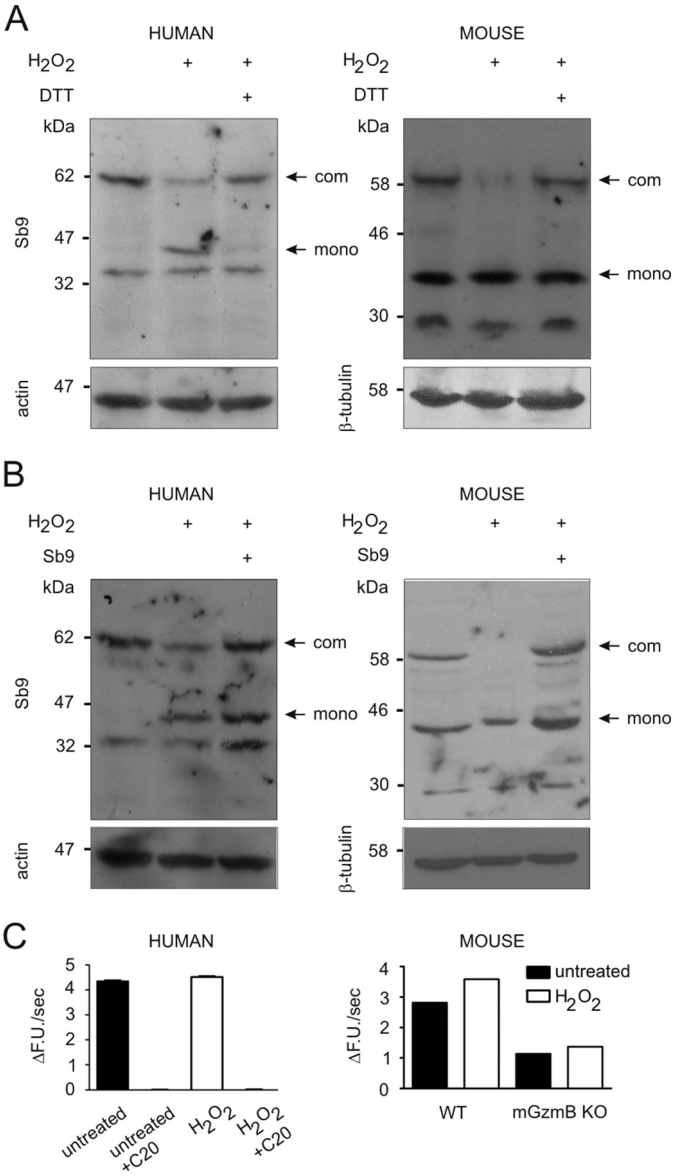

FIGURE 4. **The Sb9-GzmB interaction is reversibly inhibited by ROS acting on Sb9.** *A*, complex formation between human Sb9 and GzmB in YT cells or mouse Sb9 and GzmB in primary CTL. The cells treated with 500 μM H_2O_2 for 30 min were lysed in Nonidet P-40 with or without 100 μM DTT. *B*, complex formation between Sb9 and GzmB in human or mouse cells treated with 500 μM H_2O_2 for 30 min and lysed in Nonidet P-40 with or without 125 ng of recombinant Sb9 added. Samples were resolved via 10% SDS-PAGE and analyzed by sequential immunoblotting for human Sb9 (R12, 1:1000) and actin (1:1000) or mouse Sb9 (1:1000) and β-tubulin (1:2000). *Arrows* and labels indicate the Sb9/GzmB complex (*com*) and unbound Sb9 (*mono*). *C*, GzmB activity in H_2O_2-treated or untreated cells lysed in Triton X-100 and assessed via cleavage of quenched fluorescence peptide substrates (change in fluorescence units (*FU*)/s). Activity in human YT cells was measured using Abz-IEPDSGSQ[K-dnp], and a GzmB inhibitor (C20) was added to parallel samples to check cleavage specificity. Assays of mouse CTL GzmB used Abz-LEYDLGAL[K-dnp] are shown. Analysis of CTL from GzmB KO mice established background cleavage levels.

these results clearly indicate that Sb9 but not GzmB is affected by ROS.

Oxidation of the P1′ and P2′ Cys Residues Is Sufficient for Inhibition of Human Sb9—Sb9 contains residues susceptible to oxidation (Arg, Lys, His, Pro, Met, and Cys), which could be modified, thus preventing its interaction with GzmB. However, we focused on Cys because it is by far the most sensitive amino acid to oxidation, and there are 11 Cys residues present in the body and RCL of Sb9. Currently, there is no Sb9 structure to reliably predict which residues are exposed to the environment. A proteomics approach was therefore employed to identify exposed Cys residues in Sb9. Recombinant human Sb9 was treated with the alkylating agent iodoacetimide, then digested by trypsin or chymotrypsin, and analyzed by mass spectrometry. The resulting tryptic and chymotryptic peptides collectively contained all 11 of the Cys residues in Sb9. The only consistently alkylated Cys residues were three in the RCL at P6 (Cys^{335}), P1′ (Cys^{341}), and P2′ (Cys^{342}), as well as one at the base of the molecule between strand 2A and helix E (Cys^{98}) (data not shown).

Given that Cys^{98} falls in a region of the molecule not implicated in serpin stability, protease binding or conformational change, we postulated that oxidation of the Cys residues in the RCL is more likely to affect function. To test whether oxidative modification to the Sb9 RCL alters its properties and interaction with GzmB, four model quenched fluorescence peptide substrates resembling the human Sb9 RCL from P4-P5′ were synthesized. (We chose not to include P6 because it is not conserved in Sb9.) These peptides differed at the P1′ and P2′ positions, containing two Cys residues (WT), a single Cys to Ser substitution at either position, or a double Cys to Ser substitution (Fig. 5*A*). Our previous work has shown that mutation of the P1′ and P2′ residues in the Sb9 RCL does not affect its interaction with GzmB (33); hence we expected that GzmB would cleave the peptides equally well under reducing conditions. All peptides were treated with either 5 mM 2-ME or with 100 μM H_2O_2 and then exposed to human GzmB. As anticipated, GzmB efficiently cleaved each peptide under reducing conditions. However, under oxidizing conditions, cleavage of the WT Sb9 peptide containing two Cys residues was abolished. By contrast, oxidation had no effect on cleavage of the peptides containing either a P1′ or P2′ Ser residue (Fig. 5*A*). This was unexpected, because it suggests that oxidation of *both* Cys residues in the Sb9 RCL is required to prevent cleavage by GzmB. It also demonstrates that the redox status of the methionine residue in the RCL has no bearing on the ability of GzmB to interact with Sb9.

The P1′ and P2′ Residues in Human Sb9 Form a Vicinal Disulfide Bond—To identify the form of oxidative modification occurring, reduced and oxidized forms of the human WT Sb9 peptide substrate (peptide 1) were analyzed by mass spectrometry. The oxidized form of the peptide was 2 Da lighter than the reduced peptide, consistent with the loss of two hydrogen atoms. This indicates that a vicinal disulfide bond forms between the adjacent Cys residues in the peptide (Fig. 5*B*). However, given that Sb9 contains other Cys residues, it was necessary to confirm that the vicinal disulfide bond forms in the context of the entire protein. To investigate this, recombinant human Sb9 was exposed to H_2O_2, digested by trypsin, and analyzed by mass spectrometry. The same sample was then reduced by DTT and reanalyzed to determine whether the tryptic peptide containing the RCL sequence displayed an altered mass. The mass of the peptide containing the RCL sequence increased by 2 Da on treatment with DTT, indicating that a

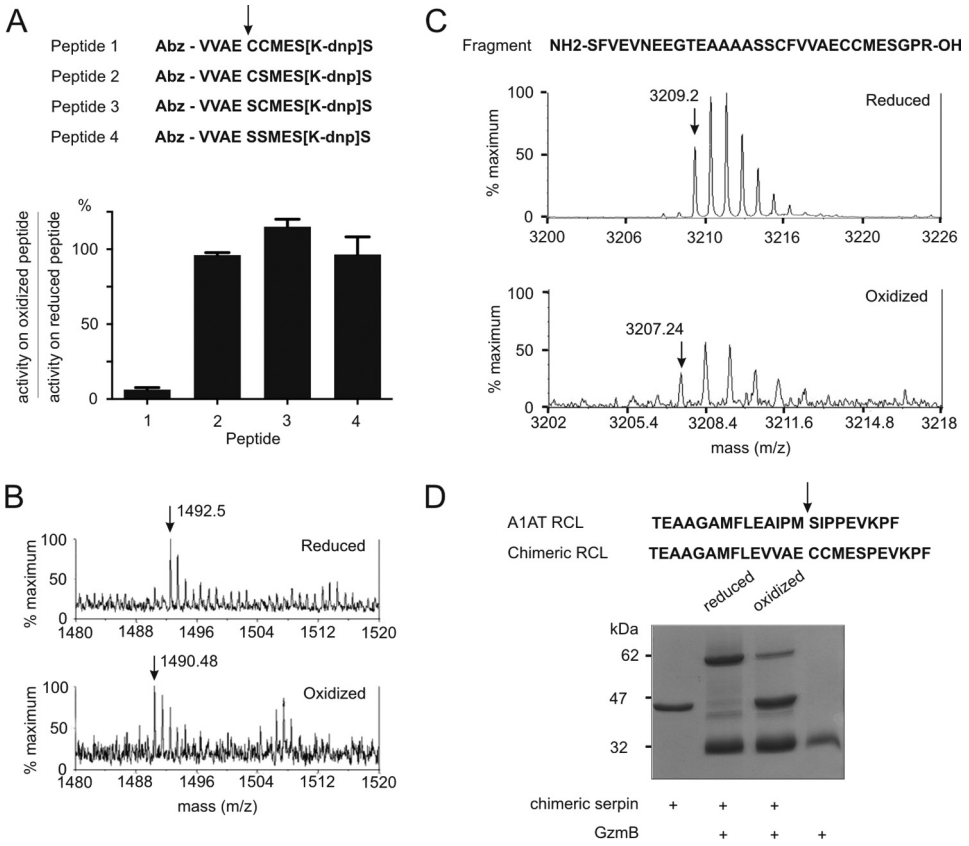

FIGURE 5. **Oxidation of the human Sb9 RCL causes vicinal disulfide bond formation and prevents cleavage by GzmB.** *A*, sequences of the four quenched fluorescence substrate peptides based on the Sb9 RCL. An *arrow* indicates the GzmB cleavage point. GzmB cleavage of oxidized peptides was compared with cleavage of reduced peptides. The *error bars* indicate S.D. from two independent experiments. *B*, mass spectrometry analysis of peptide 1 under reducing or oxidizing conditions. *C*, mass spectra of a tryptic fragment containing the RCL from human Sb9, under reducing or oxidizing conditions. Oxidized Sb9 was generated by dialysis against 500 μM H_2O_2, prior to trypsin digestion and analysis. The fragments were then treated with 100 μM DTT to generate reduced samples for analysis. *D*, comparison of the RCLs of A1AT and the Sb9/A1AT chimeric serpin. Coomassie R250-stained 10% SDS-PAGE gel showing the interaction between reduced or oxidized forms of the chimeric serpin and human GzmB (40 min at 37 °C).

vicinal disulfide bond had formed between the P1′ and P2′ Cys residues when the intact protein was oxidized (Fig. 5*C*).

To demonstrate that oxidation of the RCL is sufficient to prevent Sb9 from inhibiting GzmB, a chimeric serpin was constructed. The P4-P3′ residues of the RCL of the prototype serpin A1AT were replaced with the P4-P5′ residues of the human Sb9 RCL. Because serpin tertiary structure is highly conserved, this chimeric serpin should be capable of inhibiting GzmB (successful RCL swaps between serpins have been reported previously (40)). Furthermore, A1AT has only one (buried) Cys residue, so the chimera should be insensitive to oxidation outside the RCL.

The Sb9-A1AT chimeric serpin was expressed in and purified from *P. pastoris.* Under reducing conditions, almost all of the chimeric serpin complexed with GzmB, demonstrating that it has conventional inhibitory activity (Fig. 5*D*). By contrast, complex formation markedly decreased under oxidizing conditions, indicating that the interaction between the hybrid serpin and hGzmB had been disrupted (Fig. 5*D*). This demonstrates that oxidation of the Sb9 RCL is necessary and sufficient to prevent its interaction with hGzmB.

Mutation of the P1′ and P2′ Cys Residues to Ser Protects Human Sb9 Activity—To determine whether mutation of the P1′ and P2′ Cys residues renders Sb9 resistant to oxidative inactivation, both residues were mutated to Ser in a new construct. It is known that mutation of either the P1′ or P2′ residues to alanine has no impact on the Sb9-hGzmB interaction and that a P1′ substitution to Ser also has no effect (33). To ensure that substitution of both Cys residues to Ser has no effect on the interaction between Sb9 and GzmB, recombinant WT Sb9 protein and the mutant (Sb9 SS) protein were purified from *P. pastoris* and assessed for inhibition of GzmB under standard (mildly reducing) conditions (32). The SI for the interaction between Sb9 SS and GzmB was ~1, the same as the SI for the WT Sb9-GzmB interaction (Fig. 6*A*). The association constant (k_{ass}), a measure of the rate of complex formation, was also comparable for WT Sb9 and the SS mutant (Fig. 6*A*), confirming that conversion of the P1′ or P2′ residues to Ser has no effect on Sb9 inhibitory function.

Recombinant WT and mutant Sb9 proteins were then dialyzed against TBS containing either 100 μM 2-ME or 500 μM H_2O_2 and incubated with excess GzmB to facilitate complex formation. Under reduced conditions both WT Sb9 and the mutant efficiently bound GzmB, as complex was evident in both samples (Fig. 6*B*). By contrast, complex formation between WT Sb9 and GzmB was abolished under oxidizing conditions, whereas the interaction between the SS mutant and GzmB was unaffected (Fig. 6*B*). Thus, mutation of the P1′ and

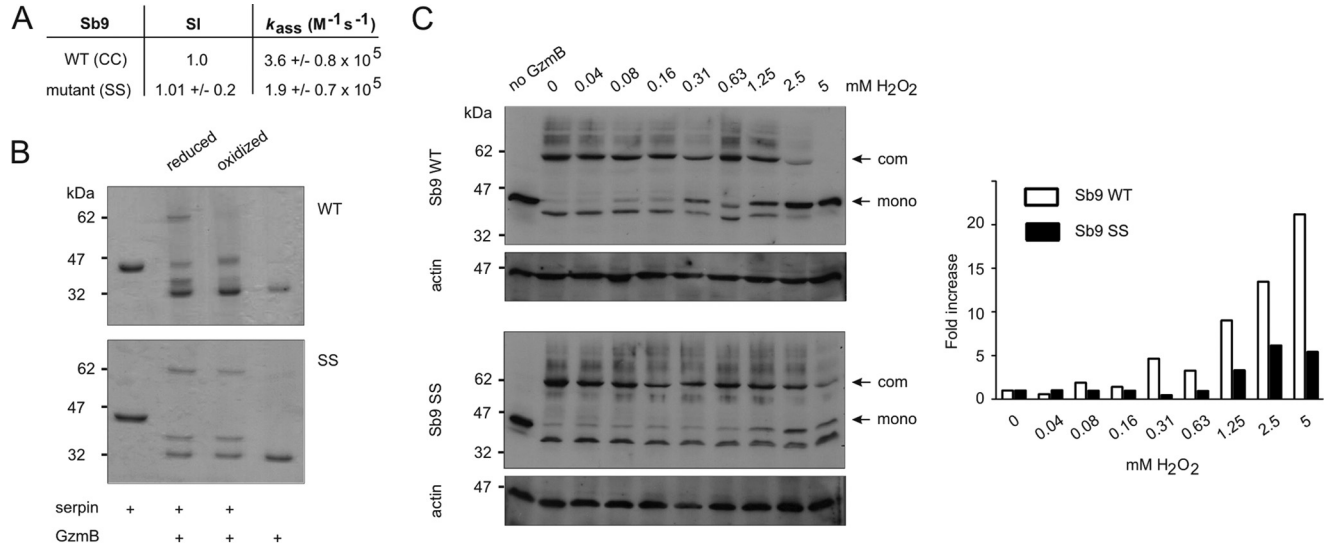

FIGURE 6. **Substitution of the human Sb9 RCL P1′ and P2′ Cys residues with Ser renders it resistant to ROS inactivation.** *A*, kinetic parameters of the interaction between GzmB and WT Sb9 or the Sb9 P1-P1′ double mutant (SS): the SI and association rate constant (k_{ass}). SI value for WT Sb9 is taken from (33). *B*, complex forming ability (*com*) of GzmB with reduced or oxidized forms of WT Sb9 or the SS mutant (at 37 °C for 10 min). Shown is a 10% SDS-PAGE gel stained with Coomassie R250. *C*, Jurkat cells transduced with either WT or SS forms of Sb9 were exposed to the indicated concentrations of H_2O_2 for 30 min. The cells were lysed in Nonidet P-40 buffer containing recombinant GzmB, and samples were resolved via 10% SDS-PAGE. Uncomplexed Sb9 (*mono*) was assessed by immunoblotting and densitometry using antibody 7D8 (1:100) and normalized to actin (1:1000).

P2′ residues is sufficient to prevent oxidative inactivation of Sb9.

Many oxidative modifications to proteins occurring *in vivo* involve other components besides ROS, and can be transient. For example, in glutathiolation a reversible disulfide bond forms between glutathione and an exposed Cys residue under oxidizing conditions (41). To ascertain whether mutation of the Sb9 P1′ and P2′ residues prevents its inactivation by ROS in a cellular environment, Sb9 and the SS mutant were expressed in the SB9- and GzmB-negative human $CD4^+$ T cell line, Jurkat E6.1, via lentivirus transduction. The viral transcriptional unit also contained an internal ribosomal entry site linking Sb9 to a dsRed reporter, so dsRed is produced whenever Sb9 is synthesized. The dsRed reporter was used to sort transduced cells into populations expressing similar levels of Sb9 via flow cytometry (data not shown). Immunoblotting demonstrated that Sb9 in these transduced cells does not form complex with any endogenous protease (for example, Fig. 6*C*, *first lane*) and that both Sb9 and the SS mutant were fully functional as indicated by all the population moving into complex when recombinant GzmB was added to cell extracts (for example, Fig. 6*C*, *second lane*).

To test whether the Sb9 SS mutant resists oxidative inactivation *in vivo*, the Jurkat E6.1 cells expressing Sb9 WT or SS mutant were exposed to increasing concentrations of H_2O_2 and lysed in the presence of recombinant GzmB. The cell extracts were analyzed by immunoblotting for Sb9. Uncomplexed WT Sb9 was absent in untreated cells but was evident in 80 μM H_2O_2 and increased as H_2O_2 concentrations rose. Complexes decreased and were completely absent at 5 mM H_2O_2 (Fig. 6*C*). By contrast, increases in uncomplexed Sb9 SS were only evident from 1250 μM H_2O_2, and complexes still formed in 5 mM H_2O_2 (Fig. 5*C*). This demonstrates that conversion of the Cys residues in the Sb9 RCL to Ser protects against oxidative modification in cells. Given that WT Sb9 is intrinsically more susceptible to oxidative damage than the SS mutant, these findings strongly suggest that the evolutionary conservation of the Cys residues in the Sb9 RCL serves a functional purpose.

Mutation of the P1 and P1′ Cys Residues in Mouse Sb9 Also Renders It Resistant to Oxidation—The RCL of mouse Sb9 differs from human Sb9 in that GzmB cleaves *between* the two Cys residues rather than adjacent to them (8). In other words, the Cys residues provide the P1-P1′ bond in this RCL. This difference could alter the susceptibility of mouse Sb9 to oxidative modification, compared with human Sb9.

Under reducing conditions, *in vitro* mouse Sb9 is fully functional, as indicated by the movement of all the serpin into complex with GzmB (Fig. 7*A*). To investigate whether oxidation of the Cys residues in the mouse Sb9 RCL influences complex formation by preventing cleavage by GzmB, fluorescence-quenched peptide substrates were synthesized to model the mouse Sb9 RCL. These peptides had either the P1′ or both Cys residues substituted by Ser (Fig. 7*B*). The peptides were treated with either 2-ME or H_2O_2 and then exposed to mouse GzmB, and the cleavage activity was measured. Mass spectrometry analysis of the reduced peptides showed that cleavage occurred at the predicted positions (data not shown). Like human Sb9, oxidized mouse Sb9 WT peptide was not cleaved by GzmB. Oxidation of the P1 Cys residue alone partially prevented cleavage by GzmB, whereas the cleavage of the peptide containing two Ser residues was essentially unaffected by oxidation (Fig. 7*B*). The effect of oxidation of the P1′ Cys alone was not investigated. These data suggest that an inactivating vicinal disulfide bond can also be formed in the mouse Sb9 RCL when both Cys residues are present and that the P1 Cys is also susceptible to oxidation.

Both Cys residues in the mouse Sb9 RCL were mutated to Ser residues (SS mutant) to test whether they are required for oxidative inhibition of the serpin in cells. Jurkat cell lines expressing either WT mouse Sb9 or the SS mutant were generated, treated with increasing concentrations of H_2O_2, and then lysed

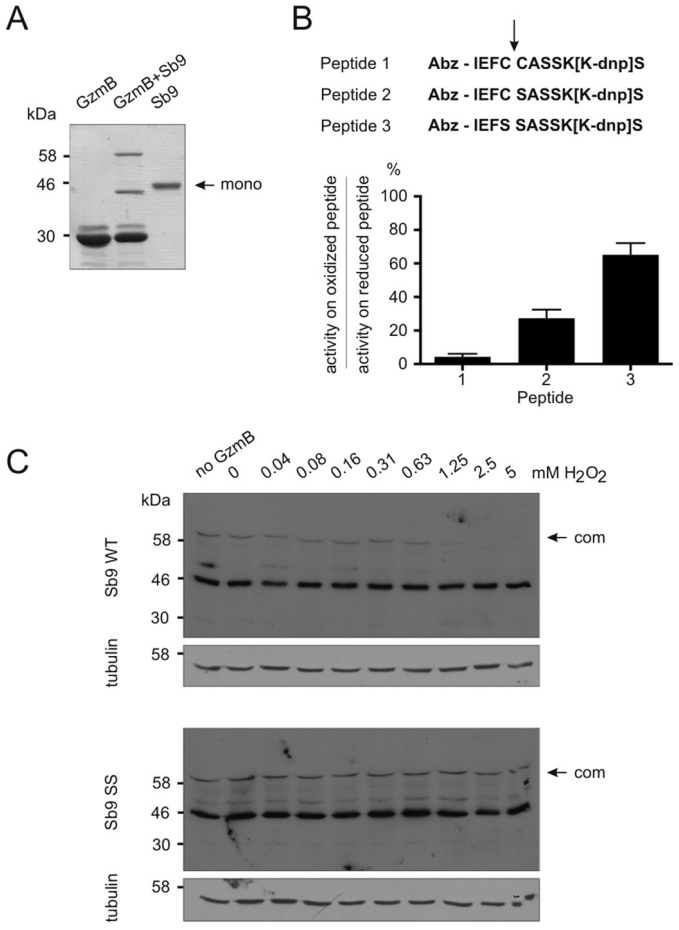

FIGURE 7. **Mouse Sb9 is also inactivated by ROS acting on the RCL Cys pair.** *A*, Coomassie R250-stained 10% SDS-PAGE gel showing the interaction between reduced recombinant mouse Sb9 and mouse GzmB. An *arrow* indicates uncleaved, uncomplexed serpin (*mono*). *B*, sequences of quenched fluorescence substrate peptides based on the mouse Sb9 RCL. An *arrow* indicates the GzmB cleavage point. GzmB cleavage of oxidized peptides in 11 mM H_2O_2 was compared with cleavage of reduced peptides in 90 mM 2-ME. The *error bars* indicate S.D. from two independent experiments. *C*, substitution of P1 and P1′ Cys by Ser renders Sb9 resistant to ROS inactivation in cells. Jurkat cells transduced with either the WT or SS forms of mouse Sb9 were exposed to indicated concentrations of H_2O_2 for 30 min. The cells were lysed in Nonidet P-40 LB containing recombinant mouse GzmB and resolved via 10% SDS-PAGE. Complex formation (*com*) was assessed by immunoblotting for Sb9 (1:1000) compared with β-tubulin (1:2000).

in the presence of mouse GzmB. As predicted, there was a noticeable decrease in the amount of complex formation between WT mouse Sb9 and GzmB at the higher concentrations of H_2O_2 (Fig. 7*C*). In comparison, there was no difference in the amount of complex formed between the SS mutant and GzmB at any of the concentrations of H_2O_2 used or in the untreated sample (Fig. 7*C*). This indicates that the susceptibility of mouse Sb9 to oxidative modification is due to the P1 and P1′ Cys residues in the RCL.

Discussion

GzmB is important for CL killing of infected or otherwise abnormal cells (42). An additional role for GzmB is emerging in mediating the death of immune cells via fratricide or suicide to limit life spans and prevent immune pathology (14, 17, 18). In the suicide mechanism, we have previously proposed that LMP liberates GzmB, which enters the cytosol of the host cell and has the potential to initiate apoptosis. Interplay between cytosolic GrB and Sb9 determines how long individual CLs can survive (19). We hypothesize that metabolic stress following activation or target cell interactions (both processes involving ROS) continually releases GrB from CL lysosomes into the cytosol. As CLs proliferate and with every target encountered and destroyed, the cytosolic GrB to Sb9 ratio in the cell increases. When the amount of GrB in the cytosol exceeds the amount of functional Sb9, the cell dies. During CL activation, GrB expression—but not Sb9 expression—markedly increases, suggesting that the probability of GrB-driven suicide increases as the CL matures. It also follows that CLs containing many lysosomes and the most GrB, *i.e.* potentially hyperactive cells with high risk of causing collateral damage to surrounding tissue, would die first, lowering the potential for immune damage. CLs not killed by this mechanism would still be subject to removal by death ligands or factor withdrawal.

We have shown here that ROS are associated with receptor-mediated LMP and GzmB-driven death of activated and working CLs and participate in a conserved mechanism of controlling Sb9. Oxidative inactivation of Sb9 occurs via formation of a vicinal disulfide bond in the RCL, which prevents GzmB from cleaving the P1-P1′ bond. We propose that ROS-mediated suppression of Sb9 increases susceptibility of the CL to GzmB-mediated death, ensuring that old or overactive cells are removed from the system and adding another layer of protection against immune pathology. It is a responsive mechanism that does not depend on the (down) regulation of Sb9 protein synthesis or increased protein turnover to lower the threshold for GzmB-mediated death. The reversible nature of the disulfide bond means that if ROS levels drop before the threshold is reached, Sb9 functionality can be recovered, and the cell will survive.

It is likely that rodent Sb9 is more sensitive to ROS inactivation than human Sb9, as indicated by the larger proportion of inactive Sb9 in mouse CTL (Fig. 3*B*). (Under ideal conditions *in vitro*, mouse Sb9 is fully active and shifts into complex with mouse GzmB (Fig. 7*A*).) This may reflect the fact that the Cys pair in mouse Sb9 comprises the P1-P1′ residues and that oxidation of the P1 Cys alone decreases efficiency of GzmB cleavage. Susceptibility to oxidation may explain our previous reports of relatively poor interaction between mouse GzmB and Sb9 *in vitro*, exemplified by a SI of 5 (7, 8). If more effective antioxidants (*e.g. tris*(2-carboxyethyl)phosphine) are used during preparation and analysis of recombinant mouse Sb9, the SI improves to 2.[4]

The model ROS used in our study, H_2O_2, is naturally produced by immune cells; however, the range of ROS that can mediate modification of Sb9 under physiological conditions is unclear. The primary exogenous sources of ROS are granulocytes and macrophages, which release oxidants into the extracellular space (44). This increases the local concentration of extracellular ROS, which can enter CLs and influence their differentiation and function, as well as increasing their susceptibility to apoptosis (25, 45). Endogenous ROS in CLs are derived

[4] M. Mangan, unpublished data.

from mitochondria as a metabolic by-product and from enzymes such as NADPH oxidase, which produce ROS essential for cell signaling (21, 22). Levels of ROS increase from both these sources on activation and are required for proliferation and differentiation of naïve cells into effector cells: by contrast, the absence of ROS from either source reduces cytokine secretion and proliferation (22, 46, 47). It is likely that a major source of ROS generated in NK cells by receptor ligation derives from mitochondria, as indicated by the cytoprotective effect of the superoxide dismutase mimetic, MnTBAP (Fig. 1*C*).

Beyond immune cells, our observations reconcile conflicting observations about the protective effect of Sb9 in cancer. Sb9 is expressed in endothelial tumors, lymphomas, and leukemias and has been proposed to protect neoplastic cells from CLs (10, 48). Sb9-positive cells resist killing by GzmB/perforin *in vitro*, as well killing by CLs (6, 10, 49). However, this appears to be cell type-dependent, because Sb9-positive lymphomas are sensitive to killing (50). In clinical studies, a correlation between (high) Sb9 expression and poor prognosis for cancer patients has been reported (51), but other studies report no such correlation (52–54). Neoplastic cells produce ROS through signaling enzymes and from mitochondria because of increased metabolic demand (55, 56). High levels of ROS would inactivate Sb9 and increase susceptibility to CLs. Differing ROS levels may partly explain the varying susceptibility of Sb9-expressing cancer cells to CLs and the inconsistent correlation between Sb9 expression and prognosis.

Oxidation-sensitive residues are found in the RCLs of other intracellular serpins, suggesting that ROS-mediated regulation of activity may not be restricted to Sb9. For example, the mouse intracellular serpin Serpina3g (Spi2A), an inhibitor of cathepsin B, has two Cys residues in the RCL and is susceptible to oxidation *in vitro* (57). Interestingly, alteration in the balance between cathepsin B and Spi2A influences mammary gland involution through a process involving LMP-mediated death. An increase in cathepsin B and a decrease in Spi2A are associated with LMP-mediated liberation of cathepsin B into the cytosol and epithelial cell death (58). Although such changes are attributed to STAT3-mediated transcriptional regulation, our results suggest that inactivation of Spi2A by ROS might also contribute to this process.

In other examples, inhibition of neutrophil elastase by monocyte/granulocyte SERPINB1 is prevented by alkylation of the serpin, indicating that modification of the Cys residue in RCL interferes with its interaction with cognate protease. SERPINB6, which inhibits cathepsin G, also contains oxidation-sensitive residues in the RCL (59, 60). Neutrophils and macrophages express both SERPINB1 and SERPINB6 and produce large amounts of ROS as part of the antibacterial response, as well as reactive nitrogen species, which are used as signaling molecules (reviewed in Ref. 61). Either ROS or reactive nitrogen species may inactivate SERPINB1 and SERPINB6 on stimulation of these cells and limit their life span by increasing susceptibility to LMP- and protease-mediated death. Lysosomal enzymes are also heavily implicated in signaling events in neutrophils, including the liberation of neutrophil elastase necessary for the formation of neutrophil extracellular traps (62). Neutrophil extracellular traps are formed from cellular components, particularly histones, and are an important part of antibacterial defense mediated by neutrophils (63). Oxidative inhibition of SERPINB1 might facilitate neutrophil extracellular trap formation by preventing its inhibition of cytosolic neutrophil elastase.

Finally, our work has practical implications. For example, purified NK cells are increasingly used in adoptive immunotherapy for cancer (64): stabilizing functional Sb9 levels through judicious use of antioxidants should improve NK cell viability by minimizing LMP/GzmB-mediated cell death. Conversely, clinical induction of LMP in GzmB-positive extranodal T cell and NK cell lymphomas (43) may offer an alternative treatment strategy to induce cancer cell death.

Conclusion

Sb9 is regulated by a conserved, ROS-mediated, reversible modification of the RCL. Formation of a vicinal disulfide bond between conserved cysteines, comprising or adjacent to the P1 residue, prevents cleavage by GzmB, which is an essential step in the serpin inhibitory mechanism. ROS-driven suppression of Sb9 activity may sensitize cells to GzmB-mediated suicide and contribute to lymphocyte homeostasis.

Author Contributions—P. I. B. conceived and coordinated the study. M. S. J. M. performed and analyzed the experiments shown in Figs. 3–7. C. H. B. carried out pilot studies and performed and analyzed the experiments shown in Figs. 1 and 2. C. H. produced the chimeric serpin and human Sb9. D. K. produced human GzmB and performed bioinformatic and kinetic analyses. D. L. S. performed proteomics analysis. A. Y. M. produced recombinant mouse GzmB. P. E. T. synthesized quenched fluorescence peptide substrates. The paper was written by P. I. B., M. S. J. M., and C. H. B. All authors reviewed the results and approved the final version of the manuscript.

Acknowledgments—We thank Dr. A. Rizzitelli for constructing pLOX-dsRed; J. Ung for pLOX-dsRed-hSb9; A. Giousoh for assistance with construction of the chimeric serpin gene; and Dr. S. Bottomley and Dr. R. Pike for advice on serpin kinetic analysis.

References

1. Silverman, G. A., Whisstock, J. C., Bottomley, S. P., Huntington, J. A., Kaiserman, D., Luke, C. J., Pak, S. C., Reichhart, J. M., and Bird, P. I. (2010) Serpins flex their muscle: I. putting the clamps on proteolysis in diverse biological systems. *J. Biol. Chem.* **285,** 24299–24305
2. Whisstock, J. C., Silverman, G. A., Bird, P. I., Bottomley, S. P., Kaiserman, D., Luke, C. J., Pak, S. C., Reichhart, J. M., and Huntington, J. A. (2010) Serpins flex their muscle: II. Structural insights into target peptidase recognition, polymerization, and transport functions. *J. Biol. Chem.* **285,** 24307–24312
3. Owen, M. C., Brennan, S. O., Lewis, J. H., and Carrell, R. W. (1983) Mutation of antitrypsin to antithrombin: α1-antitrypsin Pittsburgh (358 Met leads to Arg), a fatal bleeding disorder. *N. Engl. J. Med.* **309,** 694–698
4. Taggart, C., Cervantes-Laurean, D., Kim, G., McElvaney, N. G., Wehr, N., Moss, J., and Levine, R. L. (2000) Oxidation of either methionine 351 or methionine 358 in α1-antitrypsin causes loss of anti-neutrophil elastase activity. *J. Biol. Chem.* **275,** 27258–27265
5. Sun, J., Bird, C. H., Sutton, V., McDonald, L., Coughlin, P. B., De Jong, T. A., Trapani, J. A., and Bird, P. I. (1996) A cytosolic granzyme B inhibitor related to the viral apoptotic regulator cytokine response modifier A is present in cytotoxic lymphocytes. *J. Biol. Chem.* **271,** 27802–27809
6. Bird, C. H., Sutton, V. R., Sun, J., Hirst, C. E., Novak, A., Kumar, S., Trapani,

J. A., and Bird, P. I. (1998) Selective regulation of apoptosis: the cytotoxic lymphocyte serpin proteinase inhibitor 9 protects against granzyme B-mediated apoptosis without perturbing the Fas cell death pathway. *Mol. Cell. Biol.* **18,** 6387–6398
7. Sun, J., Ooms, L., Bird, C. H., Sutton, V. R., Trapani, J. A., and Bird, P. I. (1997) A new family of 10 murine ovalbumin serpins includes two homologs of proteinase inhibitor 8 and two homologs of the granzyme B inhibitor (proteinase inhibitor 9). *J. Biol. Chem.* **272,** 15434–15441
8. Kaiserman, D., Bird, C. H., Sun, J., Matthews, A., Ung, K., Whisstock, J. C., Thompson, P. E., Trapani, J. A., and Bird, P. I. (2006) The major human and mouse granzymes are structurally and functionally divergent. *J. Cell Biol.* **175,** 619–630
9. Classen, C. F., Bird, P. I., and Debatin, K. M. (2006) Modulation of the granzyme B inhibitor proteinase inhibitor 9 (PI-9) by activation of lymphocytes and monocytes in vitro and by Epstein-Barr virus and bacterial infection. *Clin. Exp. Immunol.* **143,** 534–542
10. Medema, J. P., de Jong, J., Peltenburg, L. T., Verdegaal, E. M., Gorter, A., Bres, S. A., Franken, K. L., Hahne, M., Albar, J. P., Melief, C. J., and Offringa, R. (2001) Blockade of the granzyme B/perforin pathway through overexpression of the serine protease inhibitor PI-9/SPI-6 constitutes a mechanism for immune escape by tumors. *Proc. Natl. Acad. Sci. U.S.A.* **98,** 11515–11520
11. Zhang, M., Park, S.-M., Wang, Y., Shah, R., Liu, N., Murmann, A. E., Wang, C.-R., Peter, M. E., and Ashton-Rickardt, P. G. (2006) Serine protease inhibitor 6 protects cytotoxic T cells from self-inflicted injury by ensuring the integrity of cytotoxic granules. *Immunity* **24,** 451–461
12. Ansari, A. W., Temblay, J. N., Alyahya, S. H., and Ashton-Rickardt, P. G. (2010) Serine protease inhibitor 6 protects iNKT cells from self-inflicted damage. *J. Immunol.* **185,** 877–883
13. Azzi, J., Skartsis, N., Mounayar, M., Magee, C. N., Batal, I., Ting, C., Moore, R., Riella, L. V., Ohori, S., Abdoli, R., Smith, B., Fiorina, P., Heathcote, D., Bakhos, T., Ashton-Rickardt, P. G., and Abdi, R. (2013) Serine protease inhibitor 6 plays a critical role in protecting murine granzyme B-producing regulatory T cells. *J. Immunol.* **191,** 2319–2327
14. Devadas, S., Das, J., Liu, C., Zhang, L., Roberts, A. I., Pan, Z., Moore, P. A., Das, G., and Shi, Y. (2006) Granzyme B is critical for T cell receptor-induced cell death of type 2 helper t cells. *Immunity* **25,** 237–247
15. Salti, S. M., Hammelev, E. M., Grewal, J. L., Reddy, S. T., Zemple, S. J., Grossman, W. J., Grayson, M. H., and Verbsky, J. W. (2011) Granzyme B regulates antiviral CD8+ T cell responses. *J. Immunol.* **187,** 6301–6309
16. Loebbermann, J., Thornton, H., Durant, L., Sparwasser, T., Webster, K. E., Sprent, J., Culley, F. J., Johansson, C., and Openshaw, P. J. (2012) Regulatory T cells expressing granzyme B play a critical role in controlling lung inflammation during acute viral infection. *Mucosal. Immunol.* **5,** 161–172
17. Ida, H., Nakashima, T., Kedersha, N. L., Yamasaki, S., Huang, M., Izumi, Y., Miyashita, T., Origuchi, T., Kawakami, A., Migita, K., Bird, P. I., Anderson, P., and Eguchi, K. (2003) Granzyme B leakage-induced cell death: a new type of activation-induced natural killer cell death. *Eur. J. Immunol.* **33,** 3284–3292
18. Laforge, M., Bidère, N., Carmona, S., Devocelle, A., Charpentier, B., and Senik, A. (2006) Apoptotic death concurrent with CD3 stimulation in primary human CD8+ T lymphocytes: a role for endogenous granzyme B. *J. Immunol.* **176,** 3966–3977
19. Bird, C. H., Christensen, M. E., Mangan, M. S., Prakash, M. D., Sedelies, K. A., Smyth, M. J., Harper, I., Waterhouse, N. J., and Bird, P. I. (2014) The granzyme B-SerpinB9 axis controls the fate of lymphocytes after lysosomal stress. *Cell Death Differ.* **21,** 876–887
20. Aits, S., and Jäättelä, M. (2013) Lysosomal cell death at a glance. *J. Cell Sci.* **126,** 1905–1912
21. Jackson, S. H., Devadas, S., Kwon, J., Pinto, L. A., and Williams, M. S. (2004) T cells express a phagocyte-type NADPH oxidase that is activated after T cell receptor stimulation. *Nat. Immunol.* **5,** 818–827
22. Sena, L. A., Li, S., Jairaman, A., Prakriya, M., Ezponda, T., Hildeman, D. A., Wang, C.-R., Schumacker, P. T., Licht, J. D., Perlman, H., Bryce, P. J., and Chandel, N. S. (2013) Mitochondria are required for antigen-specific T cell activation through reactive oxygen species signaling. *Immunity* **38,** 225–236
23. Hildeman, D. A. (2004) Regulation of T-cell apoptosis by reactive oxygen species. *Free Rad. Biol. Med.* **36,** 1496–1504
24. Michalek, R. D., Nelson, K. J., Holbrook, B. C., Yi, J. S., Stridiron, D., Daniel, L. W., Fetrow, J. S., King, S. B., Poole, L. B., and Grayson, J. M. (2007) The requirement of reversible cysteine sulfenic acid formation for T cell activation and function. *J. Immunol.* **179,** 6456–6467
25. Hansson, M., Asea, A., Ersson, U., Hermodsson, S., and Hellstrand, K. (1996) Induction of apoptosis in NK cells by monocyte-derived reactive oxygen metabolites. *J. Immunol.* **156,** 42–47
26. Tiscornia, G., Singer, O., and Verma, I. M. (2006) Production and purification of lentiviral vectors. *Nat. Protocols* **1,** 241–245
27. Hirst, C. E., Buzza, M. S., Bird, C. H., Warren, H. S., Cameron, P. U., Zhang, M., Ashton-Rickardt, P. G., and Bird, P. I. (2003) The intracellular granzyme B inhibitor, proteinase inhibitor 9, is up-regulated during accessory cell maturation and effector cell degranulation, and its overexpression enhances CTL potency. *J. Immunol.* **170,** 805–815
28. Trapani, J. A., Browne, K. A., Dawson, M., and Smyth, M. J. (1993) Immunopurification of functional Asp-ase (natural killer cell granzyme B) using a monoclonal antibody. *Biochem. Biophys. Res. Commun.* **195,** 910–920
29. Northfield, S. E., Roberts, K. D., Mountford, S. J., Hughes, R. A., Kaiserman, D., Mangan, M., Pike, R. N., Bird, P. I., and Thompson, P. E. (2010) Synthesis of "difficult" fluorescence quenched substrates of granzyme C. *Int. J. Pept. Res. Ther.* **16,** 159–165
30. Kaiserman, D., Hitchen, C., Levina, V., Bottomley, S. P., and Bird, P. I. (2011) Intracellular production of recombinant serpins in yeast. *Methods Enzymol.* **501,** 1–12
31. Sun, J., Bird, C. H., Buzza, M. S., McKee, K. E., Whisstock, J. C., and Bird, P. I. (1999) Expression and purification of recombinant human granzyme B from *Pichia pastoris*. *Biochem. Biophys. Res. Commun.* **261,** 251–255
32. Horvath, A. J., Lu, B. G., Pike, R. N., and Bottomley, S. P. (2011) Methods to measure the kinetics of protease inhibition by serpins. *Methods Enzymol.* **501,** 223–235
33. Sun, J., Whisstock, J. C., Harriott, P., Walker, B., Novak, A., Thompson, P. E., Smith, A. I., and Bird, P. I. (2001) Importance of the P4′ residue in human granzyme B inhibitors and substrates revealed by scanning mutagenesis of the proteinase inhibitor 9 reactive center loop. *J. Biol. Chem.* **276,** 15177–15184
34. Bird, C. H., Rizzitelli, A., Harper, I., Prescott, M., and Bird, P. I. (2010) Use of granzyme B-based fluorescent protein reporters to monitor granzyme distribution and granule integrity in live cells. *Biol. Chem.* **391,** 999–1004
35. Benarafa, C., and Remold-O'Donnell, E. (2005) The ovalbumin serpins revisited: perspective from the chicken genome of clade B serpin evolution in vertebrates. *Proc. Natl. Acad. Sci. U.S.A.* **102,** 11367–11372
36. Kaiserman, D., and Bird, P. I. (2005) Analysis of vertebrate genomes suggests a new model for clade B serpin evolution. *BMC Genomics* **6,** 167
37. Williams, M. S., and Kwon, J. (2004) T cell receptor stimulation, reactive oxygen species, and cell signaling. *Free Rad. Biol. Med.* **37,** 1144–1151
38. Miki, H., and Funato, Y. (2012) Regulation of intracellular signalling through cysteine oxidation by reactive oxygen species. *J. Biochem.* **151,** 255–261
39. Willoughby, C. A., Bull, H. G., Garcia-Calvo, M., Jiang, J., Chapman, K. T., and Thornberry, N. A. (2002) Discovery of potent, selective human granzyme B inhibitors that inhibit CTL mediated apoptosis. *Bio. Med. Chem. Lett.* **12,** 2197–2200
40. Schick, C., Brömme, D., Bartuski, A. J., Uemura, Y., Schechter, N. M., and Silverman, G. A. (1998) The reactive site loop of the serpin SCCA1 is essential for cysteine proteinase inhibition. *Proc. Natl. Acad. Sci. U.S.A.* **95,** 13465–13470
41. Hill, B. G., and Bhatnagar, A. (2012) Protein S-glutathiolation: Redox-sensitive regulation of protein function. *J. Mol. Cell. Cardiol.* **52,** 559–567
42. Afonina, I. S., Cullen, S. P., and Martin, S. J. (2010) Cytotoxic and non-cytotoxic roles of the CTL/NK protease granzyme B. *Immunol. Rev.* **235,** 105–116
43. Bajor-Dattilo, E. B., Pittaluga, S., and Jaffe, E. S. (2013) Pathobiology of T-cell and NK-cell lymphomas. *Best Pract. Res. Clin. Haematol.* **26,** 75–87
44. Briggs, R. T., Karnovsky, M. L., and Karnovsky, M. J. (1975) Cytochemical demonstration of hydrogen peroxide in polymorphonuclear phagosomes. *J. Cell Biol.* **64,** 254–260
45. Gelderman, K. A., Hultqvist, M., Pizzolla, A., Zhao, M., Nandakumar,

K. S., Mattsson, R., and Holmdahl, R. (2007) Macrophages suppress T cell responses and arthritis development in mice by producing reactive oxygen species. *J. Clin. Invest.* **117,** 3020–3028
46. Devadas, S., Zaritskaya, L., Rhee, S. G., Oberley, L., and Williams, M. S. (2002) Discrete generation of superoxide and hydrogen peroxide by T cell receptor stimulation. *J. Exp. Med.* **195,** 59–70
47. Tatla, S., Woodhead, V., Foreman, J. C., and Chain, B. M. (1999) The role of reactive oxygen species in triggering proliferation and IL-2 secretion in T cells. *Free Rad. Biol. Med.* **26,** 14–24
48. Buzza, M. S., Hirst, C. E., Bird, C. H., Hosking, P., McKendrick, J., and Bird, P. I. (2001) The granzyme B inhibitor, PI-9, is present in endothelial and mesothelial cells, suggesting that it protects bystander cells during immune responses. *Cell. Immunol.* **210,** 21–29
49. Bots, M., Kolfschoten, I. G., Bres, S. A., Rademaker, M. T., de Roo, G. M., Krüse, M., Franken, K. L., Hahne, M., Froelich, C. J., Melief, C. J., Offringa, R., and Medema, J. P. (2005) SPI-CI and SPI-6 cooperate in the protection from effector cell-mediated cytotoxicity. *Blood* **105,** 1153–1161
50. Godal, R., Keilholz, U., Uharek, L., Letsch, A., Asemissen, A. M., Busse, A., Na, I.-K., Thiel, E., and Scheibenbogen, C. (2006) Lymphomas are sensitive to perforin-dependent cytotoxic pathways despite expression of PI-9 and overexpression of bcl-2. *Blood* **107,** 3205–3211
51. Bladergroen, B. A., Meijer, C. J., ten Berge, R. L., Hack, C. E., Muris, J. J., Dukers, D. F., Chott, A., Kazama, Y., Oudejans, J. J., van Berkum, O., and Kummer, J. A. (2002) Expression of the granzyme B inhibitor, protease inhibitor 9, by tumor cells in patients with non-Hodgkin and Hodgkin lymphoma: a novel protective mechanism for tumor cells to circumvent the immune system? *Blood* **99,** 232–237
52. Classen, C. F., Ushmorov, A., Bird, P., and Debatin, K. M. (2004) The granzyme B inhibitor PI-9 is differentially expressed in all main subtypes of pediatric acute lymphoblastic leukemias. *Haematologica* **89,** 1314–1321
53. de Hooge, A. S., Berghuis, D., Santos, S. J., Mooiman, E., Romeo, S., Kummer, J. A., Egeler, R. M., van Tol, M. J., Melief, C. J., Hogendoorn, P. C., and Lankester, A. C. (2007) Expression of cellular FLICE inhibitory protein, caspase-8, and protease inhibitor-9 in Ewing sarcoma and implications for susceptibility to cytotoxic pathways. *Clin. Cancer Res.* **13,** 206–214
54. Muris, J. J., Meijer, C. J., Cillessen, S. A., Vos, W., Kummer, J. A., Bladergroen, B. A., Bogman, M. J., MacKenzie, M. A., Jiwa, N. M., Siegenbeek van Heukelom, L. H., Ossenkoppele, G. J., and Oudejans, J. J. (2004) Prognostic significance of activated cytotoxic T-lymphocytes in primary nodal diffuse large B-cell lymphomas. *Leukemia* **18,** 589–596
55. Cairns, R. A., Harris, I. S., and Mak, T. W. (2011) Regulation of cancer cell metabolism. *Nat. Rev. Cancer* **11,** 85–95
56. Kobayashi, C. I., and Suda, T. (2012) Regulation of reactive oxygen species in stem cells and cancer stem cells. *J. Cell Physiol.* **227,** 421–430
57. Morris, E. C., Dafforn, T. R., Forsyth, S. L., Missen, M. A., Horvath, A. J., Hampson, L., Hampson, I. N., Currie, G., Carrell, R. W., and Coughlin, P. B. (2003) Murine serpin 2A is a redox-sensitive intracellular protein. *Biochem. J.* **371,** 165–173
58. Hughes, K., and Watson, C. J. (2012) The role of Stat3 in mammary gland involution: cell death regulator and modulator of inflammation. *Horm. Mol. Biol. Clin. Investig.* **10,** 211–215
59. Scott, F. L., Hirst, C. E., Sun, J., Bird, C. H., Bottomley, S. P., and Bird, P. I. (1999) The intracellular serpin proteinase inhibitor 6 is expressed in monocytes and granulocytes and is a potent inhibitor of the azurophilic granule protease, cathepsin G. *Blood* **93,** 2089–2097
60. Cooley, J., Takayama, T. K., Shapiro, S. D., Schechter, N. M., and Remold-O'Donnell, E. (2001) The serpin MNEI inhibits elastase-like and chymotrypsin-like serine proteases through efficient reactions at two active sites. *Biochemistry* **40,** 15762–15770
61. Fialkow, L., Wang, Y., and Downey, G. P. (2007) Reactive oxygen and nitrogen species as signaling molecules regulating neutrophil function. *Free Rad. Biol. Med.* **42,** 153–164
62. Papayannopoulos, V., Metzler, K. D., Hakkim, A., and Zychlinsky, A. (2010) Neutrophil elastase and myeloperoxidase regulate the formation of neutrophil extracellular traps. *J. Cell Biol.* **191,** 677–691
63. Brinkmann, V., Reichard, U., Goosmann, C., Fauler, B., Uhlemann, Y., Weiss, D. S., Weinrauch, Y., and Zychlinsky, A. (2004) Neutrophil extracellular traps kill bacteria. *Science* **303,** 1532–1535
64. Lapteva, N., Szmania, S. M., van Rhee, F., and Rooney, C. M. (2014) Clinical grade purification and expansion of natural killer cells. *Crit. Rev. Oncogenesis* **19,** 121–132